Symkom 2014 **Open Access**

Michał Lipian*, Maciej Karczewski, and Krzysztof Olasek

Sensitivity study of diffuser angle and brim height parameters for the design of 3 kW Diffuser Augmented Wind Turbine

DOI 10.1515/eng-2015-0034

Received December 28, 2014; accepted May 18, 2015

Abstract: The Diffuser Augmented Wind Turbine (DAWT) is an innovative mean to increase the power harvested by wind turbine. By encompassing the rotor with a diffuser-shaped duct it is possible to increase the flow speed through the turbine by about 40-50%. The study presents the development of a numerical model and its validation by the experiments performed in the wind tunnel of the Institute of Turbomachinery, TUL. Then, the numerical model is used for the geometry sensitivity study to optimize the shape of a diffuser. The paper presents that the DAWT technology has the potential to even double the power outcome of wind turbine when compared to a bare rotor version.

Keywords: Diffuser Augmented Wind Turbine (DAWT); small wind turbines; wind energy; numerical flow simulation; computational fluid dynamics (CFD); Particle Image Velocimetry (PIV); simulation-experiment integration

1 Introduction

An increasing demand for reliable green energy source leads to a vast development in wind power sector. However, optimisation of rotor geometry may only be done within the so-called Betz limit, stating that no more than about 60% of wind's kinetic energy may be harvested and converted into a mechanical power on the shaft. In practice, the conversion rate is on average 30% for majority of the Horizontal Axis Wind Turbines (HAWTs). One possible solution to increase energy production rate over this limit is to force more air to move through the working section of turbine. This can be achieved by equipping the rotor with a diffusing channel around it, thus creating a shrouded wind turbine.

The Shrouded Wind Turbine concept may be traced back to as early as 1970s. Gilbert and Foreman [1] mainly concentrated on a long divergent channel structure with a turbine placed inside, while Igra [2] proved that a compact shroud may be equally interesting. However, the idea has not remained commercially exploited until the results of numerous studies performed at Japanese Kyushu University were published (see for example [3, 4]). The research conducted at Kyushu University proposed a more compact form of a shroud, called "wind lens", in which the outlet of a diffuser is equipped with a brim. The experiments showed numerous advantages of this solution: significant rise in the power output, increase of safety by housing the rotor or decrease of acoustic noise [3, 5].

The general operation principle of a shrouded wind turbine may be explained with fluid mechanics principles. The brim is an obstacle for the oncoming flow that creates a low-pressure zone downstream. The low-pressure zone draws more air into the channel to equalize the pressure gradient. By increasing the mass flow through the diffuser, a significant flow acceleration is observed at the inlet of a divergent duct where the turbine is placed [6–8]. This theory becomes insufficient to explain the flow acceleration in the diffuser outlet region that is observed for diffuser angles of about 20° and higher, a phenomenon that the "wind lens" compact designs are based on.

In order to broaden knowledge of flow nature around brimmed diffusers and, further, a Diffuser-Augmented Wind Turbine (DAWT), a series of numerical analysis were conducted. Based on an experimentally validated numerical model, a sensitivity study of two parameters describing the geometry of an isolated diffuser was made in order to identify a design which can further increase the flow velocity through the channel. Results of this study are presented in the following document.

2 Numerical model

Figure 1 presents the numerical domain developed for the purpose of the simulations. The proposed size was deter-

***Corresponding Author: Michał Lipian:** Institute of Turbomachinery, Faculty of Mechanical Engineering, Łódź University of Technology, E-mail: michal.lipian@p.lodz.pl

Maciej Karczewski, Krzysztof Olasek: Institute of Turbomachinery, Faculty of Mechanical Engineering, Ł´odź University of Technology

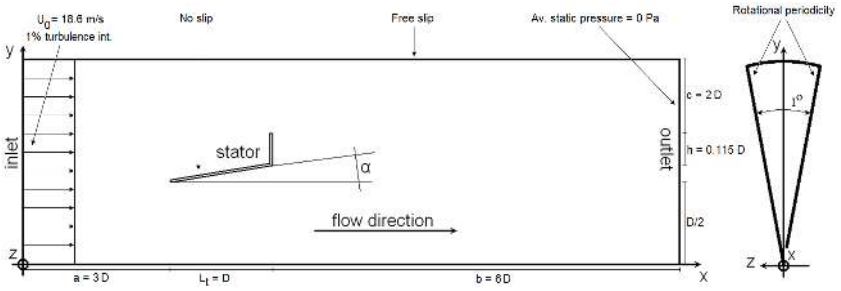

Figure 1: Simulation domain of the proposed numerical model.

mined via a model independence study. To limit the size of the computational task the domain encompassed an axisymmetric 1° section of a flow field, where rotational periodicity boundary condition around the X axis was imposed. The diffusing channel was placed at the distance equal to three diameters from the inlet cross-section. A combination of boundary conditions was used to mimic the flow in the Institute of Turbomachinery (IMP) wind tunnel. Hence, the free slip wall condition (no through flow allowed) was used to adhere to an open wind tunnel test section and the outlet cross-section imposing a perpendicular outflow, where an ambient pressure of 101325 Pa was used. The flow was treated as isothermal, steady-state type with air treated as an ideal gas. A low (1%) turbulence intensity was set at the inlet, which corresponds to a value measured in IMP wind tunnel (see for example [9]). The turbulence model independence test including the SST and $k - \varepsilon$ closure were performed and will be presented in Chapter 3. Care was taken to assure that near-wall mesh elements provide y+ values around 1 in order to use the ω-based equation to compute boundary layer flows. For places where this was not possible, a velocity profile from flat plate experiment was imposed.

The key geometrical parameters of the modelled diffuser are grouped in Table 1. The inlet diameter-based Reynolds number was calculated to be $6.61 \cdot 10^5$ and corresponds to a small ducted 3 kW turbine operating at wind speed of 4 m/s (annual average wind speed at 2/3 of territory of Poland 10 m above ground, [10]). In the wind tunnel measurement, the model in a smaller scale was tested to limit the blockage coefficient to 0.05.

The proposed mesh was envisaged so as to favour the regions of interest: diffuser boundary layer and inside region and generally the region downstream the brim-diffuser structure. The mesh was swept face-to-face around the X axis. Meshing statistic parameters are listed in Table 2, while the general overview of the mesh is visible in Figure 2.

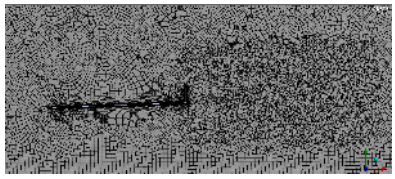

Figure 2: Zoom of the mesh near the diffuser wall.

3 Numerical model validation

3.1 Experimental stand

Experimental study has been carried out in the subsonic wind tunnel at the Institute of Turbomachinery at the Lodz University of Technology. The investigated diffuser model was placed in the free stream inside the test section (downstream the circular wind tunnel outlet nozzle). To limit the blockage effect of the model, an open test section was used with the model size frontal area equal to 5% of the contraction nozzle area supplying the air into the test area.

Particle Image Velocimetry (PIV) and pneumatic probe measurements have been made.

3.2 PIV measurements

PIV experimental equipment, that has been used, consisted of the following main components:

- double-pulse Nd:YAG laser from Litron (1200 mJ max output, 4 ns pulse duration, 1064/532 nm wavelength),
- arm with optical system redirecting laser beam to a desired position,
- laser sheet optics (cylindrical lens f=-20),
- two PIV cameras Imager Pro x 4M from LaVision (2048x2048 pixels),
- Nikkor camera lenses (24-85 mm, f2.8).

Table 1: Details of the diffuser model used in the numerical analysis.

	feature value	
diffuser feature	experiment	CFD simulation
inlet diameter D	0.135 m	0.540 m
length L_t	1	
outlet diameter d_2	1.074 D	
brim height h	0.115 D	
diffuser angle 2α (derived parameter)	4.25°	
Reynolds number based on D	1.65E+005	6.61E+005

Table 2: Mesh parameters.

parameter	(average) value	standard deviation
number of nodes	612411	-
number of elements	459951	-
element quality	0.663	0.302
aspect ratio	9.9	36.72
skewness	0.136	0.123

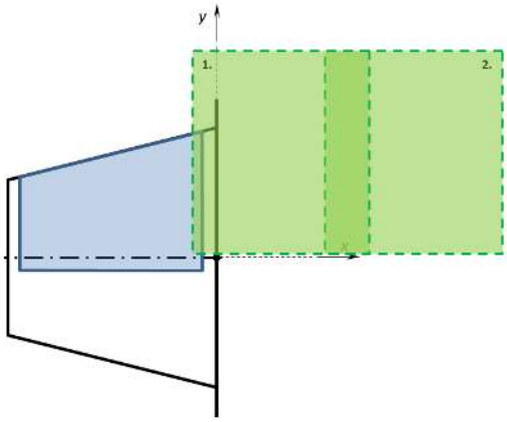

Figure 3: Arrangement of measurement planes.

PIV measurement plane was aligned with the flow direction. It was positioned vertically and passed through the axis of a channel, perpendicular-wise to the brim of diffuser. Two cameras in 2D measurement mode were used in order to obtain large velocity flow field downstream the DAWT (see Figure 3).

3.3 Pneumatic measurements

To supplement the PIV tests, pneumatic measurements have been performed. Pitot-static pressure probe connected to a pressure difference transducer was used. By measuring the pressure difference between output signals of probes (total and static pressure), dynamic pressure was

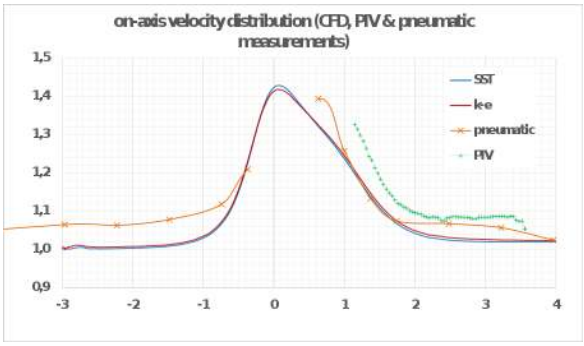

Figure 4: On-axis velocity distribution.

obtained allowing for the calculation of the flow velocity. Measurement system was equipped with an automatic data acquisition system in order to perform multiple measurement for one location of the probe. Information about the temperature have been gathered with a thermocouple, while an ambient pressure was measured with a mercury-based barometer.

3.4 Comparison of results with the experimental data

Velocity distribution at the locations, where pressure measurements have been taken, are presented in Figures 4 and 5. A comparison of results obtained by means of numerical simulations with two different turbulence models as well as experimental data from PIV and pneumatic probe measurements are shown. No data was recorded by PIV in the region upstream the diffuser thus only pneumatic measurements and CFD results are compared for that zone in Figure 4.

The axial velocity distributions presented in Figure 4 reveal a quantitative agreement between the CFD and the experimental methods. The dashed linesmark the area where a diffuser was placed. The PIV measurements are not available inside the channel but pressure probe mea-

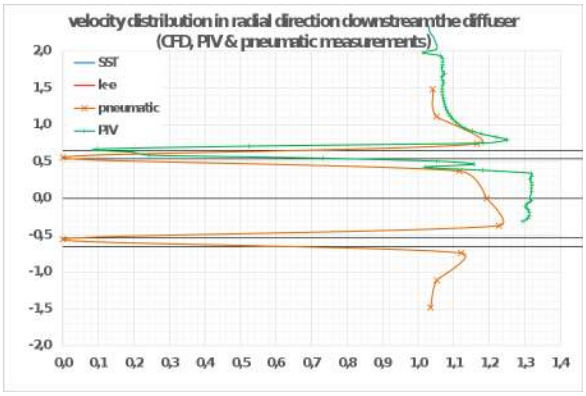

Figure 5: Velocity distribution downstream the diffuser at a distance x/D=1.1 (refer to Figure 4 for location)

surements confirm the observed velocity trends. The simulation results are indifferent despite that two varying turbulence models were used and clearly show an over 40% of velocity rise at the diffuser inlet (x/D=0). Velocity gradually returns to the free stream value at the distance of two diameters downstream the diffuser. The simulation results are about 6% lower than the experimental ones. This may be attributed to the fact that the reference value of U_0 was measured directly at the outlet of the wind tunnel nozzle, at a location laden with flow turbulence. The tunnel is of blow-down type and, at the moment of the experiment, was equipped with a nozzle of a crude design which could additionally intensify local flow unsteadiness. Tests of a new nozzle, based on Witoszynski formula, are planned shortly, and this phenomena should not be visible in the future studies. Because the difference observed between experimental and numerical results is quite consistent in the flow domain presented in Figure 4, it could have been reduced by using an appropriate correction. However, it was not judged as crucial for the numerical model used in the sensitivity study since the character of the measured flow is nearly exactly mimicked by the simulation. This proves the representative character of the model.

A very good quantitative agreement between simulation and the experiment was found downstream the diffuser, where some of the measurements were made inside the wakes. The inner dashed lines mark the diffuser outlet diameter, while the outer dashed lines locate the ends of the brim. Therefore, the numerical models are validated for flows laden with aerodynamic wakes. For further analysis, the SST turbulence model was used. Figure 6 compares the distribution of flow velocity in the domain, as seen in the PIV experiment and in the simulation. The two images present very good qualitative correlation of both cases concerning the size and location of the observed flow phenomena.

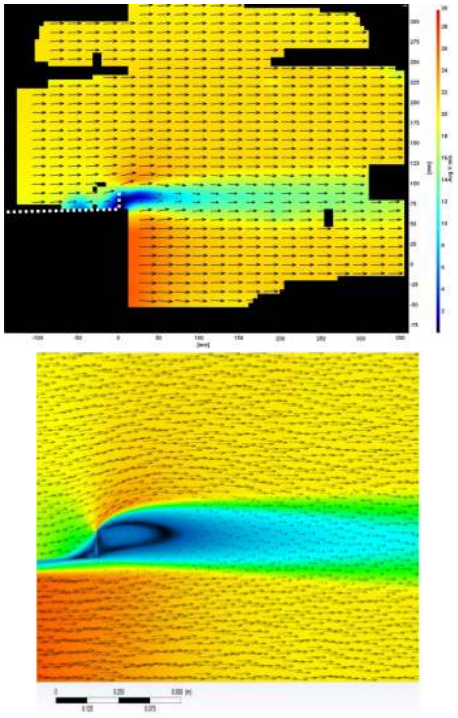

Figure 6: Velocity contour plot and vectors: PIV (L) versus simulation (R) results.

4 Numerical model for DAWT simulation

The described numerical model was used in a sensitivity study process of a diffuser geometry for 3 kW Diffuser-Augmented Wind Turbine with inlet diameter of D = 2.5 m. To simulate the rotor's presence an actuator disc was placed at the distance of 0.05 m from the diffuser inlet in place, where the maximum velocity occurs (refer to Figure 4). The disc was allowed to rotate at the rotational speed of 150 rpm, while a pressure drop of 7 Pa was imposed across its boundaries to simulate the rotor load. Figure 7 presents the other boundary conditions used in the study: inlet velocity was equal to 6 m/s with inlet turbulence Tu = 5%. In total 48 geometries were examined, covering 3 different brim heights (0.1D, 0.3D and 0.5D) and 16 diffuser angles (from 0°to 30°with interval 2°).

In order to determine the imposed pressure drop across the rotor plane, the experimental results as presented by Abe and Ohya [11] were used. Pressure coefficient c_p difference due to the load exerted on the rotor by

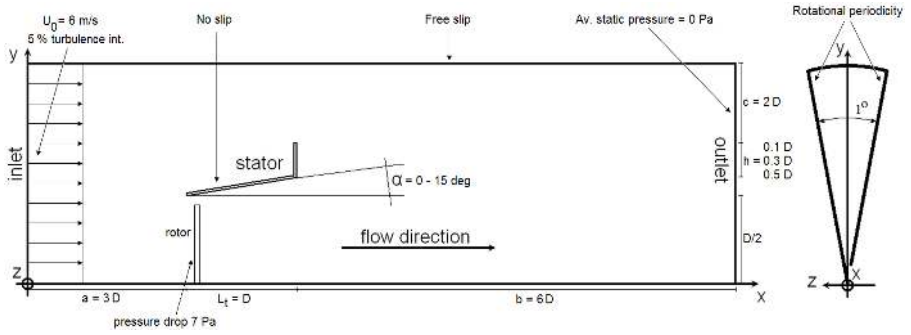

Figure 7: General view of the simulation domain for the calculations in rotor presence.

the fluid was determined by using the plot data available in Figure 8. Abe and Ohya [11] reported that the c_p drops from about -0.78 to -1.22 producing $\Delta c_p = 0.44$ when loading coefficient $C_t = 0.2$. The following definition of the loading coefficient was proposed by [11]:

$$C_t = \frac{p - 1 - p_2}{\frac{1}{2}\rho \cdot U_2^2} \tag{1}$$

which differs from standard C_t definition, and where p1 is the pressure immediately upstream the rotor plane, p_2 and U_2 denote pressure and velocity immediately downstream the rotor. The aforementioned values of c_p difference were next employed in the standard formula defining the pressure coefficient:

$$p_1 - p_2 = \Delta = \Delta c_p \cdot \frac{1}{2}\rho \cdot U_0^2, \tag{2}$$

where U_0 describes free stream velocity of 5 m/s at which Abe and Ohya [11] performed tests in the wind tunnel, air density was assumed as in own CFD simulations (ρ = 1.185kg/m3). The obtained numerical result is about Δp = 7 Pa. Next, the Δp value was imposed across the actuator disc model in own CFD simulations of the small DAWT (D = 2.5 m). The results of this study are visible in Figure 8 as well and correspond well to the reference data, which concerns the pressure drop in rotor plane. Therefore, for the further analysis presented herein the value of Δp = 7 Pa was assumed.

The difference in quantitative relationship between the implemented model in own simulation and the experimental values is due to the existence of a sharp entry edge at the diffuser inlet. In numerical simulation this leads to the creation of sudden pressure drop, extending from the diffuser inlet to about x/D = 0.4, as visible also in Figure 8. At the same time, the experimentally investigated diffuser in [11] is not explicitly described to possess either sharp inlet edge or aerodynamically optimal inlet. The implication that this particular geometrical feature could have on the sensitivity results presented in the following sections

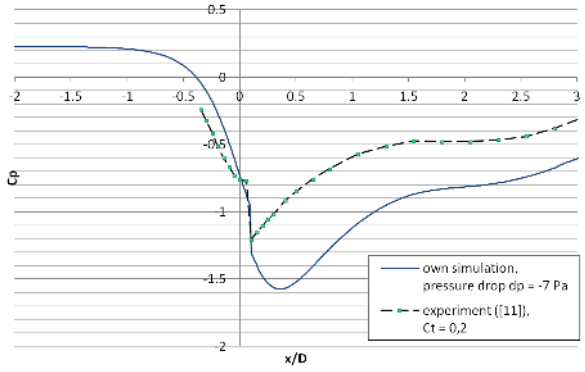

Figure 8: Streamwise distribution of pressure coefficient for experiment in [11] and own CFD simulations.

is minimal as the same numerical effect occurs in all simulations.

5 Sensitivity study of DAWT's diffuser angle and brim height

Figure 9 shows typical features of the considered flow. The velocity rise of about 50% can be observed at the turbine inlet and potentially even more at about 0.2D downstream the diffuser inlet.

The region downstream the brim is a low-pressure zone, and the flow behaviour in this region is different with varying geometry. Low brim and low diffuser angle result in creation of only small wake. Augmenting these two geometric parameters results generally in the creation of two vortices – one, nearer to the stream exiting the diffuser, directed counter clockwise, and another one – above, turning clockwise. Very high diffuser angles may result in the creation of a boundary layer separation which causes energy losses. In case of the considered flows, for angles above 26°, the boundary-layer vortices connected

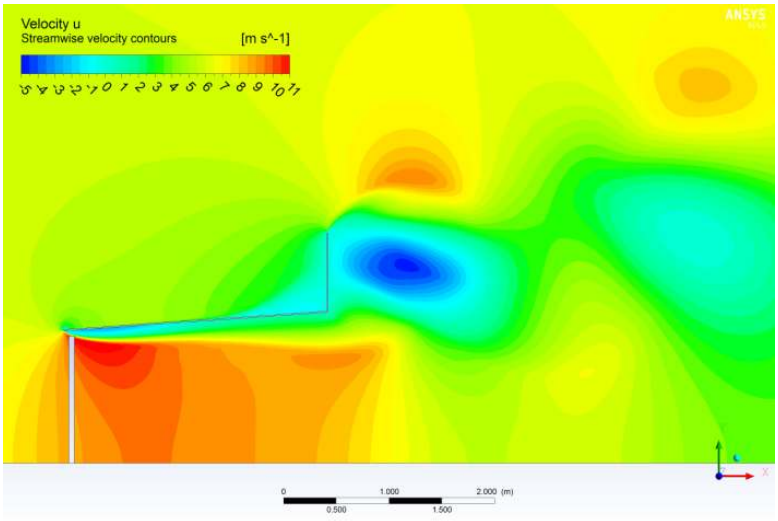

Figure 9: Velocity contour plot of flow through DAWT, D = 2.5 mm, L = D, h = 0.3D, $2\alpha = 8°$.

with the vortex behind the brim creating a massive separation zones and flow instabilities.

Figure 10 presents the results of the sensitivity study where the influence of the diffuser angle and the brim height on the velocity at the rotor inlet can be estimated. The velocities were area-averaged and then divided by the free stream value.

Generally, the test results show that the flow velocity gain, regardless of the brim height, is as high as even 1.6 for diffuser angles of about 6°. Another observation is that smaller diffuser angles favour higher brims. On the other hand, the angles from the range 18°-26°show equally satisfactory flow velocity increase. However, in these cases, the areas in which the flow accelerates are usually shifted towards the diffuser outlet where, as described earlier, larger flow separation regions form due to increasing diffuser angles. These structures may potentially amplify the vibrations of the channel and the turbine itself, presenting a challenge from a structural, control and safety points of view. The brim of reduced height is generally preferred in these cases. Despite the unsteady character of the flow, these geometries may be of significant interest, as a flow velocity rise even of magnitude 2 was observed.

The proposed rotor modelling technique assumes a constant pressure drop across the virtual rotor plane. This would not be the case in reality, especially when the geometrical changes introduced lead to the increase of the streamwise velocity at the rotor inlet (see Figure 10). Namely, the pressure drop is expected to rise according to the rise of dynamic pressure upstream the rotor. However, the DAWT geometry models in the sensitivity study were not identical as in Abe and Ohya [11] to directly impose

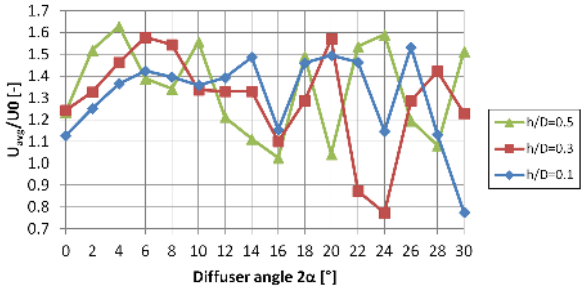

Figure 10: Comparison of averaged value of dimensionless velocity at the rotor inlet for all examined geometries.

pressure drop characteristics as based on experiment. At the time own CFD study was prepared no experiment existed to derive representative pressure drop in own model. Therefore, this point leaves place for a potential improvement in flow modelling.

For further analysis, the dimensionless streamwise velocity U/U_0 plots for angles 2α = 6°and 22°are presented in Figure 11 and Figure 12. In case of the 6°, the distribution of the axial velocity reveals that the maximum velocity in rotor plane occurs for the brim with mediocre height (h = 0.3D). Additionally, the velocity flow field downstream the DAWT is influenced by the size of the brim as the velocity plot shows the return of the exit velocity to the free stream value only in the case of the smallest brim. At a higher diffuser angle, 2α = 22°, the DAWT with the highest brim leads to a slightly higher U/U_0 ratio at rotor plane as in the case of the brim with h = 0.1D. At these diffuser angles, flow instabilities complicate interpretation of the numerical results due to its unsteady character. Nevertheless, some observations agree with the literature data. For

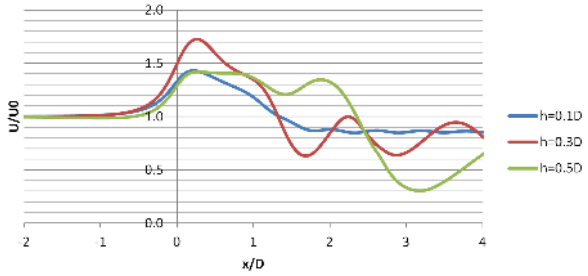

Figure 11: Streamwise flow velocity distribution for the case 2α=6°and varying brim heights.

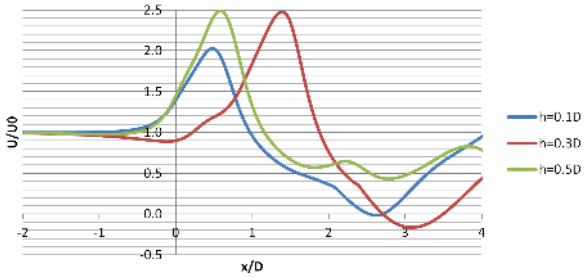

Figure 12: Streamwise flow velocity distribution for the case 2α=22°and varying brim heights.

example [11] observed higher turbine power values for diffuser angles 2α = 30°. However, computations were made at higher loading coefficient.

Furthermore, what is likewise interesting, in both cases the maximum flow acceleration is observed at locations inside the diffuser rather than directly at the inlet (x/D = 0). As the diffuser angles rise, the influence of the diffuser leading edge becomes lower with the boundary layer separations growing larger. Thus, the velocity peak zone may be shifted further downstream the diffusing channel, as seen for example in Figure 12. This may favour a second contra rotating turbine rotor to harvest the remaining energy and increase overall power production of the plant. This investigation is a subject of another scientific study conducted at the Institute of Turbomachinery, at the Lodz University of Technology.

Acknowledgement: The research leading to these results has received funding from the Polish-Norwegian Research Programme operated by the National Centre for Research and Development under the Norwegian Financial Mechanism 2009-2014 in the frame of Project Contract No. PolNor/200957/47/2013.

References

[1] Gilbert B.M., Foreman K.L., Experiments with a diffuser-augmented model wind turbine, J. Energy Resour. Technol., 1983, 105, 46–53.
[2] Igra O., Research and development for shrouded wind turbines, Energ. Convers. Manage., 1981, 21(1), 13–48.
[3] Ohya Y., Karasudani T., A Shrouded Wind Turbine Generating High Output Power with Wind-Lens Technology, Energies, 2010, 2(3), 634–649.
[4] Ohya Y., Karasudani T., Matsuura C. T., A highly efficient wind turbine with wind-lens shroud, Proceedings of 13th International Conference on Wind Engineering Amsterdam 2011
[5] Kosasih B., Tondelli A., Experimental study of shrouded micro wind turbine, Procedia Eng., 2012, 49, 92–98.
[6] White F.M., Fluid Mechanics, 6th edition, McGraw-Hill, New York, 2008
[7] Jamieson P., Innovation in wind turbine design, 1 st edition, John Wiley & Sons, Chichester, West Sussex, United Kingdom, 2011, 255–258.
[8] Kazimierski Z., Orzechowski Z., Mechanika płynów, 4th edition, Wydawnictwo Politechniki Łódzkiej, Łódź, 1979.
[9] Kulak M., Olasek K., Karczewski M., Reduction of wind tunnel turbulence intensity level by installation of a honeycomb straightener - CFD simulation vs. experiment, Proceedings of the XX Fluid Mechanics Conference KKMP2012 Gliwice 2012, ISBN 978-83-927340-8-6.
[10] Lorenc H., Atlas klimatu Polski, Instytut Meteorologii i Gospodarki Wodnej, Warszawa, 2005.
[11] Abe K., Ohya Y., An investigation of flow fields around flanged diffusers using CFD, J. Wind. Eng. Ind. Aerod., 2004, 92, 315–330.